Projected XMM Vision for MCVs

Cynthia H. James, Graziella Branduardi-Raymont and Mark Cropper

Mullard Space Science Laboratory, University College London, Holmbury St Mary, Surrey, UK

Abstract. The XMM satellite has a scientific payload of 3 EPIC and 2 RGS instruments which provide for both imaging and non-dispersive spectroscopy as well as medium-to-high resolution dispersive spectroscopy, in the soft to medium X-ray bands. The co-aligned OM adds the facility for simultaneous optical and UV studies. In this poster paper we describe the instrumental characteristics of XMM, comparing them to those of ASCA. We also forecast the expected X-ray spectra of a selection of both the Polars and Intermediate Polars by means of simulations based on ASCA model fits.

1. Introduction

XMM, carries 3 co-aligned X-ray telescopes with (to date) an unsurpassed X-ray photon collecting potential. At the focus of two of these telescopes is an RGS dispersive spectrometer and an EPIC-mos capable of both non-dispersive spectroscopy and imaging. At the focus of the third X-ray telescope is an EPIC-pn, again capable of both non-dispersive spectroscopy and imaging.

There is currently considerable interest in the physical processes associated with accretion and accretion disks. Magnetic Cataclysmic Variables (mCVs) provide us with Galactic examples of these processes in the presence of strong magnetic fields, but progress is presently limited by the data quality. The ASCA SIS is at present the facility in the X-ray wavelength band which most closely approaches the capabilities of XMM. Over the years since its launch in 1993 a number of papers have included the spectral analysis of several Polar and Intermediate Polar (IPs).

In this poster paper we make an assessment of the scientific capabilities of XMM for mCVs. We use the spectral fitting software package, XSPEC, to simulate data of several mCVs based on the parameters from the spectral model fitting of ASCA data.

2. Simulations

In order to place these simulations in context we firstly make a comparison between the ASCA SIS and the XMM RGS and EPIC cameras with respect to the instrument specifications, as given in Table 1, and their respective photon gathering efficiency, as given in Figure 1. The models used in these simulations

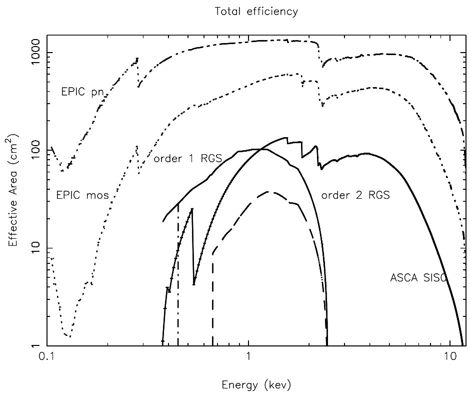

Figure 1. Comparison of effective areas between ASCA and the XMM X-ray instruments.

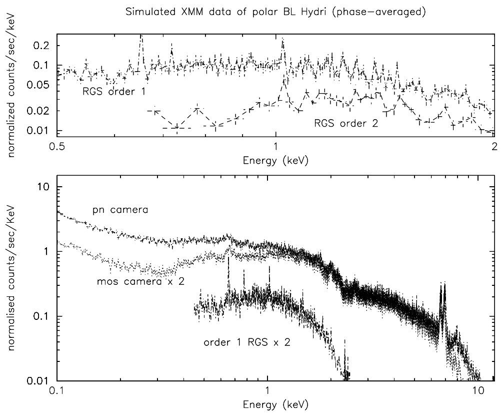

Figure 2. Simulated XMM data of the Polar BL Hydri (phase averaged), using the model parameters as given in Table 2. Top: orders 1 and 2 spectra from a single RGS. Bottom: spectra from the two RGS, the two EPIC-mos and single EPIC-pn cameras.

include both thermal bremssstralung, and optically thin MEKAL plasma (single and multi-temperature) codes, with constant and partial covering absorbers. In all cases we have limited the modelling to that which was used for the ASCA analysis. The parameters we've used for the simulations are given in Tables 2, 3 and 4. The simulated data, created by folding the models through published response matrices for each of the XMM X-ray instruments is shown in Figures 2, 3 and 4.

3. Discussion

Probably the most dramatic improvement in data quality is with respect to the effective area. This can be appreciated by comparing the normalised counts/sec/keV given by simulated EPIC camera results from BL Hyi data, Figure 2, EX Hya data, Figure 3 and AM Her data, Figure 4 with their respective results from ASCA data, Matt et al. (1998), Allan et al. (1998) and Ishida et al. (1997). Even in the case of the RGS the combined output of the first order spectra equates to that obtained from the ASCA data over its relevant wavelength range.

Figures 2 – 4 clearly demonstrate the improvement in energy resolution by the number of resolvable emission lines present in the simulated data. This is clear from a comparison of simulated spectra of BL Hyi data, Figure 2, and EX Hya data , Figure 3, with their ASCA spectra in Matt et al. (1998) and Allan et al. (1998) respectively. The underlying model fitted for AM Her is a bremsstralung continuum, hence this effect is less apparent. Another illustration is the comparison of the simulated spectra of EX Hya and BL Hyi with that

Instrument Specification	ASCA SIS	EPIC-pn	EPIC-mos	RGS order 1	RGS order 2
energy range (keV)	0.7-10.0	0.1-15.0	0.1-10.0	0.35-2.50	0.62-2.50
energy resolution (eV) @ 0.35 keV			0.443		
energy resolution (eV) @ 0.69 keV			1.44	0.84	
energy resolution (eV) @ 1.24 kev			4.32	2.38	
energy resolution (eV) @ 2.00 keV	0.18	0.08	0.08		
energy resolution (eV) @ 6.00 keV	0.20	0.13	0.08		

Table 1. Comparison of relevant ASCA and XMM instrumental specifications.

integration time	(s)	43000
flux (2-10keV)	erg cm^{-2} s^{-1}	8.0 x 10^{-12}
metal abundance	Anders & Grevesse	1.76
isothermal plasma	Single temperature Mekal (keV)	12.0
partial absorbers	nH (10^{22} cm^{-2})	3.2 x 10^{-1}
	Covering fraction	0.39

Table 2. The model and parameters values used in the simulation for BL Hyi as specified in Table 2 model 2, Matt et al. (1998).

integration time	(s)	34000
flux @ 0.6-10 keV	erg cm^{-2}s^{-1}	1.4 x 10^{-10}
isothermal plasma	4 temperature Mekal(keV)	15.4, 3.2, 1.0, 0.54
metal abundance	Allen 1973	1.0
	normalisation (10^{-2})	3.62, 3.76, 0.72, 0.67
partial absorber	nH (10^{22} cm^{-2})	0.24
	covering fraction	0.60

Table 3. The model and parameters values used in the simulation for EX Hya as specified in Table 1 spin max, Allan et al. (1998).

integration time	(s)	37000
flux @ 2-10 keV	erg cm^{-2} s^{-1}	7.2 x 10^{-11}
continuum	bremsstralung temperature (keV)	14.0
metal abundance	Anders & Ebihara	1.0
3 partial absorbers	nH (10^{22} cm^{-2})	9.0 x 10^{-3}, 2.0, 20.0
	Covering fraction	0.27, 0.22, 0.51
3 emission lines	Fe (keV)	6.40, 6.65, 6.93
	sigma (keV)	0.06, 0.04, 0.06
	total photons cm^{-2} s^{-1} 10^{-4}	1.163, 1.17, 1.131

Table 4. The model and parameters values used in the simulation for AM Her as specified spin maximum, Ishida et al. (1997).

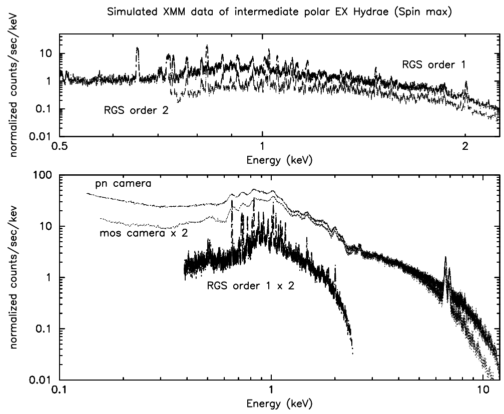

Figure 3. Simulated XMM data for IP EX Hya (spin maximum) using the model parameters as given in Table 3. Top: orders 1 and 2 spectra from a single RGS. Bottom: spectra from the two RGS, the two EPIC-mos and single EPIC-pn cameras.

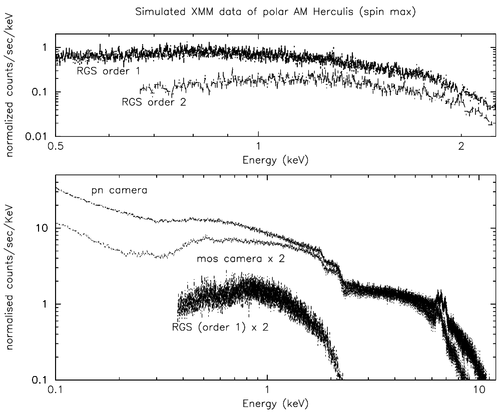

Figure 4. Simulated XMM data for polar AM Her at spin maximum using the model parameters as given in Table 4. Top: orders 1 and 2 spectra from a single RGS. Bottom: spectra from the two RGS, the two EPIC-mos and single EPIC-pn cameras.

of AM Her. All three systems show Fe emission lines in the 6.0 – 7.0 keV range. However in the latter their presence is directly attributable to the added Gaussians based on ASCA fitting parameters: these are much broader than in the first pair, where their presence is due to the metal abundance parameter in the MEKAL code model.

Finally, the resolution of the RGS first order is probably insufficient to resolve velocity shifts of the accretion flows in these systems. However, where the level of flux is relatively high, as in the case of EX Hya, then the higher resolution of the RGS 2nd order point spread function may be sufficient.

References

Allan, A., Hellier, C., & Beardmore, A. 1998, MNRAS, 295, 167

Arnaud, K.A. 1996, in Astronomical Data Analysis Software and Systems V ASP Conference Series, Vol 101

Ishida, M., Mukai, K.,& Osborne, J.P. 1994, PASP, 46, L81

Ishida, M., Matsuzaki, K., Fujimoto, R., Mukai, K.,& Osborne, J.P. 1997, MNRAS, 287, 651

Matt, G., Barcaroli, R., Belloni, T., Beuermann, K., Bonnet-Bidaud, J.M., De Martino, D., Done, C., Gansicke, B.T., Guainazzi, M., Mouchet, M.,& Mukai, K. 1998, A&A, 334, 857